Nanoparticle-mediated transgene expression of *insulin-like growth factor 1* in the guinea pig placenta differentially affects fetal liver gene expression depending on maternal nutrient status

Rebecca L. Wilson[1]*, Kendal K. Stephens[2,3], Kristin Lampe[2], Mukesh K. Gupta[4], Craig L. Duvall[4], Helen N. Jones[1,5]

[1]Department of Physiology and Functional Genomics, College of Medicine, University of Florida, Gainesville, Florida, USA 32610
[2]Department of Obstetrics and Gynecology, University of Cincinnati, Cincinnati, Ohio, USA, 45229
[3]Center for Fetal and Placental Research, Cincinnati Children's Hospital and Medical Center, Cincinnati, Ohio, USA 45229
[4] Department of Biomedical Engineering, Vanderbilt University, Nashville, TN, USA
[5]Department of Obstetrics and Gynecology, College of Medicine, University of Florida, Gainesville, Florida, USA 32610

*Corresponding Author:
Rebecca Wilson
Department of Physiology and Functional Genomics
University of Florida
Gainesville, Florida 32610
Phone: (352) 846-1503
Email: rebecca.wilson@ufl.edu

Placenta, Pregnancy, Fetal Growth Restriction, Therapeutic, Insulin-like 1 Growth Factor

Fetal growth restriction (FGR) occurs in up to 10% of pregnancies and is a leading cause of infant morbidity and mortality. Additionally, FGR has been implicated in contributing to the development of long-term health outcomes including increasing the risk for future cardiovascular and endocrine diseases. Currently, there is limited preventative strategies and no effective treatment options for FGR. To address this need, we are developing a therapeutic targeting the placenta to increase expression of human *insulin-like growth factor 1* (*hIGF-1*) and enhance placental development and function, with the goal of correcting fetal growth trajectories.

Methods Initially, an ultrasound-guided, transcutaneous, intra-placental injection of a non-viral, Texas-red conjugated polymer-based nanoparticle containing a plasmid with the *green fluorescent protein* (*GFP*) gene under the control of the placenta-specific promotors *Plac1* or *Cyp19a1* was performed to determine nanoparticle uptake and transgene expression in the guinea pig placenta. Subsequently, using the established maternal nutrient restriction (MNR) guinea pig model of FGR, placentas were treated with an unconjugated nanoparticle containing a plasmid with the *hIGF-1* gene under the *Cyp19a1* promotor at mid-pregnancy (gestational day (GD) 30-33). Five days after treatment placentas and fetal liver tissue was collected, weighed, and fixed for histology or snap-frozen for qPCR analysis of mRNA expression.

Results Histological analysis of Texas-red and GFP fluorescence in placenta and fetal liver tissue confirmed nanoparticle uptake and transgene expression and that nanoparticle was unable to cross the placenta to fetal circulation. In situ hybridization for plasmid-specific mRNA confirmed sustained *hIGF-1* expression five days after treatment. MNR resulted in 20-25% decreased fetal weight at mid-pregnancy (P<0.001) that was not changed with nanoparticle treatment (P>0.05). There was no effect of nanoparticle treatment on the volume densities of trophoblasts or fetal capillaries in the placenta (P>0.05 for both). However, treatment did reduce the interhaemal distance between the maternal blood space and fetal circulation in the MNR placentas compared to sham treated MNR placentas (P<0.001). In the fetuses, placental nanoparticle treatment increased circulating glucose by 38-50% (P<0.001) and was associated with differential changes to fetal liver mRNA expression of genes associated with gluconeogenesis. Gene expression changes were dependent on if the fetus was growth restricted or not; nanoparticle treatment: down-regulated gluconeogenesis gene expression in the normal growing fetuses but increased expression in the FGR fetuses.

Conclusions The current study shows that treatment of the guinea pig placenta with a polymer-based nanoparticle causes expression of *hIGF-1* and ultimately increases fetal glucose concentrations within five days of treatment. Furthermore, the data shows that the placenta and fetal liver respond differently to nanoparticle treatment depending on fetal growth conditions.

Graphical Abstract

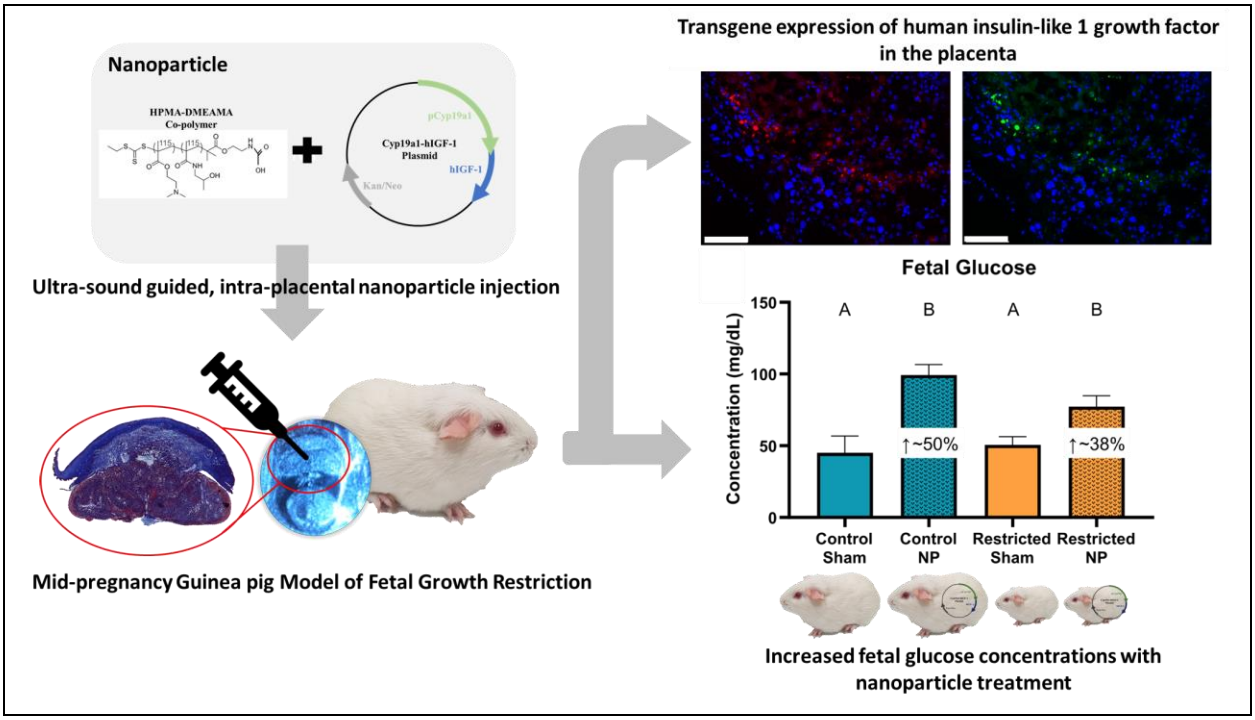

Introduction

Fetal growth restriction (FGR: estimated fetal weight <10th percentile) occurs in up to 10% of pregnancies with suboptimal fetal nutrition and uteroplacental perfusion accounting for 25-30%

of cases [1, 2]. Perinatal outcomes depend largely on the severity of FGR, however, and FGR is a leading cause of infant morbidity and mortality [3]. In addition, FGR has been implicated in contributing to the development of long-term health outcomes including increasing the risk for future cardiovascular and endocrine diseases such as diabetes [4] as well as being associated with cognitive and learning disabilities [5]. Currently, there is limited preventative strategies and no effective treatment options. However, advances in nanomedicine are allowing for the development of potential therapeutics to treat the placenta and correct fetal growth trajectories [6].

Nanoparticles are capable of exploiting existing cellular uptake mechanisms to carry and deliver drugs [7]. Furthermore, nanoparticles are capable of being created to specifically target a particular organ, thus allowing for maximized efficiency in smaller doses [8]. The placenta represents the ideal site for intervention as it is discarded after birth and thus, there are limited potential long-term consequences for maternal health. Additionally, given a large proportion of FGR cases are due to placental insufficiency, treatments actively targeted at improving placenta function is a logical approach to enabling the fetus to achieve its full growth potential. Currently, there are a number of studies being undertaken that are designed at specifically targeting the placenta to improve pregnancy outcome [9]. Furthermore, given that placental development shares similar characteristics to cancer, there is the potential the exploit knowledge from cancer research in the development of pregnancy therapies [10].

Many polymer and lipid based nanoparticles have been developed for non-viral gene therapy. Currently, we are developing the use of a polymer-based nanoparticle that facilitates non-viral gene delivery specifically to the placenta [11, 12]. Using a synthetic HPMA-DMEAMA (N-(2-hydroxypropyl) methacrylamide-2-(dimethylamino)ethyl methacrylate) diblock copolymer, complexed with a plasmid containing the human *insulin-like 1 growth factor* (*hIGF-1*) gene under the control of placenta trophoblast specific promotors (*PLAC1* and *CYP19A1*), we have shown efficient nanoparticle uptake into human syncytiotrophoblast ex vivo [12] and increased placenta expression of *hIGF-1* that is capable of maintaining fetal growth in a surgically-induced mouse model of FGR [11]. IGF-1 is a secreted protein produced by the placenta throughout pregnancy [13]. Through binding with the IGF-1 Receptor (IGF-1R), it regulates numerous aspects of placenta function including metabolism, mitogenesis, and differentiation [14]. We and others have demonstrated that increased placental expression of IGF-1 is capable of upregulating glucose and amino acid transport to the fetus and thus modulating fetal growth [15-17].

Development of a treatment for FGR is made more difficult by the lack of definitive ways to predict FGR prior to diagnosis, and as such, effective therapies must be capable of correcting the effects of existing placental dysfunction. Guinea pigs offer a unique advantage in studying the placenta, fetal development, and reproductive health as they have similar developmental milestones to humans both throughout gestation and following birth [18, 19]. Guinea pig placentas better reflect humans over other small animal species [20], exhibit deeper placental trophoblast

invasion [21], and undergo changes to the maternal hormonal profile throughout pregnancy that more closely resemble humans [22]. Additionally, non-invasive, maternal nutrient restriction (MNR) where dam food intake is restricted to 70% 4 weeks prior to pregnancy until mid-gestation and 90% thereafter, induces FGR [23, 24]. Here, we aimed to characterize placenta uptake of nanoparticle and the effects on fetal liver gene expression in the guinea pig MNR model of FGR.

Materials and Methods

Synthesis of poly(2-hydroxypropyl methacrylamide ($PHPMA_{115}$-ECT))

In a 25 mL round bottom flask equipped with a magnetic stirrer bar, ECT (4-cyano-4-(ethylsulfanylthiocarbonyl) sulfanylvpentanoic acid; 0.025 mmol, 0.006 g), HPMA (5 mmol, 0.715 g), and AIBN (2,2′-azo-*bis*-isobutyrylnitrile; 0.0025 mmol, 0.0004 g) were dissolved in DMF (dimethyl formamide; 5 mL) and sealed with septa. The solution was degassed for 30 mins by purging with ultra-high purity nitrogen and submerged into a preheated oil bath at 65 ºC. After 24 h, the crude polymerization mixture was purified through precipitation into cold diethyl ether. The pale-yellow color polymer was dried overnight under vacuum and the structure of the polymer was characterized by ^{1}H NMR spectroscopy.

Synthesis of diblock copolymer of poly(2-hydroxypropyl methacrylamide-*b*-N, N-Dimethyl aminoethyl methacrylate) ($PHPMA_{115}$-*b*-$PDMAEMA_{115}$)

RAFT (reversible addition fragmentation chain transfer) polymerization of DMEAMA was performed using $PHPMA_{115}$-ECT as a macro-CTA (chain transfer agent) and AIBN as a free radical initiator. A solution of $PHPMA_{115}$-ECT (0.031 mmol, 0.51 g), DMAEMA (4.65 mmol, 0.73 g, 0.782 mL), and AIBN (0.0031 mmol, 0.0005 g) in methanol (5 mL) was degassed for 30 minutes through purging with high purity nitrogen. To initiate the polymerization, the reaction flask was submerged in preheated oil at 70 ºC. The crude polymerization mixture was precipitated three times into cold pentane and dried under high vacuum after 24 h. The precipitated polymer was dissolved into methanol and dialyzed first against methanol for 24 h and then against deionized water for another 48 h. The dialyzed polymer was lyophilized to obtain a white powder, and formation of the diblock copolymer was confirmed by ^{1}H NMR spectroscopy.

Nanoparticle Formation

Nanoparticles were formed by complexing plasmids containing either the *green fluorescent protein* (*GFP*) or *hIGF-1* gene under control of placental trophoblast specific promotors *PLAC1* or *CYP19A1* with a non-viral $PHPMA_{115}$-b-$PDMEAMA_{115}$ co-polymer. The dialyzed polymer was resuspended in sterile water at a concentration of 10 mg/mL, then mixed with the plasmid at a ratio of 1.5 µL polymer to 1 µg plasmid, and made to a total injection volume of 200 µL with sterile phosphate buffered saline (PBS). To initially determine nanoparticle uptake and promotor recognition in the guinea pig placenta, polymer was conjugated with a Texas Red fluorophore [12].

Animal Care and Transuterine, Intra-placental Nanoparticle Injections

Female Dunkin-Hartley guinea pigs were purchased (Charles River Laboratories, Wilmington, MA) at 500-550 g and housed in a temperature-controlled facility with a 12 h light-dark cycle. Whilst acclimatizing to the facilities and for initial investigations into nanoparticle uptake in the placenta, food (LabDiet diet 5025: 27% protein, 13.5% fat, and 60% carbohydrate as % of energy) and water was provided ad libitum. Animal care and usage was approved by the Institutional Animal Care and Use Committees at Cincinnati Children's Hospital and Medical Center (Protocol number 2017-0065) and University of Florida (Protocol number 202011236).

In the initial studies to determine nanoparticle uptake and transgene expression in the guinea pig placenta, the Texas Red conjugated polymer was complexed with plasmid containing the *GFP* gene. Females (*n* = 6; 2 sham, 2 *Plac1* promotor, 2 *Cyp19a1* promotor) were time mated through daily monitoring of the estrus cycle by inspecting perforation of the vaginal membrane [25]. Ovulation was assumed to occur when the vaginal membrane was fully perforated and designated gestational day (GD) 1. Pregnancy confirmation ultrasounds were performed at GD21 and at GD30, females underwent an ultrasound-guided, transuterine, intra-placental nanoparticle injection (50 µg plasmid in 200 µL injection). Females were anaesthetized using isoflurane, their abdomen shaved and cleaned using isopropanol and the placenta for injection visualized using ultrasound. A single injection of nanoparticle was provided into the placental labyrinth as close to the visceral cavity as possible. Females were then allowed to recover in a humidicrib maintained at 37ºC before being return to their home cages. Euthanasia occurred 30 hours after injection by carbon dioxide asphyxiation followed by cardiac puncture and exsanguination. The gravid uterus was dissected and fetuses and placentas weighed. Maternal and fetal organs including heart, lungs, liver, kidney and brain were collected. These tissues, along with the placentas, were halved and either fixed in 4% w/v paraformaldehyde (PFA) or snap-frozen in liquid nitrogen and stored at -80ºC. Tissues placed in PFA were left at 4ºC until appropriately fixed, transferred to 30% w/v sucrose solution and then rapidly frozen in OCT and stored at -80ºC.

To determine the effect of nanoparticle treatment on placental function under adverse maternal conditions, females were weight and assigned to either the control diet group (C; n = 11) where food and water was provided ad libitum, or maternal nutrient restricted group (MNR/R; n = 12). MNR females were provided water ad libitum however, food intake was restricted to 70% per kilogram body weight of the C group from four weeks preconception through to mid-pregnancy (GD30), thereafter increasing to 90% (Sohlstrom 1998; Elias 2017). Time mating and pregnancy confirmation ultrasounds were performed as previously described; females not confirmed pregnant were re-mated with all females falling pregnant within three mating attempts. At GD30-33, females underwent an ultrasound-guided, transuterine, intra-placental nanoparticle injection of plasmid containing *hIGF-1* as previously described. All females were then sacrificed five days after injection (GD35-38). On the day of sacrifice, females were fasted for four hours, weighed and then euthanized as previously described. Glucose concentrations in both maternal and fetal blood was measured using a glucometer. Tissue collection was performed as previously described however, tissue placenta in PFA fixed was processed and paraffin embedded following standard

protocols. Fetal sex was determined by examination of the gonads and confirmed using PCR as previously published [26].

Fluorescent Microscopy of Nanoparticle Uptake

Placenta and fetal liver tissue from females treated with the Texas Red, *GFP* nanoparticle were assessed microscopically for nanoparticle uptake and transgene expression. 7 µm thick tissue sections were obtained, OCT was cleared by washing in ice-cold PBS, nuclei counterstained with DAPI (*Invitrogen*), and mounted using Prolong Gold Antifade mounting medium (*Invitrogen*). Texas Red and GFP fluorescence was visualized using the Nikon Eclipse Ti Inverted microscope.

In situ Hybridization for Plasmid-Specific mRNA

In situ hybridization of plasmid-specific mRNA was performed on placenta tissue treated with nanoparticle containing the *hIGF-1* plasmid to confirm sustained transgene expression five days after injection as previously described [12, 26]. Two 5 µm thick, paraffin embedded serial tissue sections were obtained. For the first section, in situ hybridization was performed using a BaseScope™ probe (*Advanced Cell Diagnostics*) custom designed to recognize the sequence between the stop codon and polyA signaling of the plasmid, following standard protocol. A section of human placenta explant treated with nanoparticle was included as a positive control. For the second section, immunohistochemistry (IHC) was performed to confirm localization of plasmid-specific mRNA in placental trophoblast cells following standard IHC protocols. Following de-waxing and rehydrating, targeted antigen retrieval was performed using boiling 1x Targeted Retrieval Solution (*Dako*) for 20 mins. Endogenous peroxidase activity was suppressed by incubating sections in 3% hydrogen peroxide for 10 mins and then sections were blocked in 10% goat serum with 1% bovine serum albumin (BSA; *Jackson ImmunoResearch*) in PBS for 1 h at room temperature. Anti-pan cytokeratin (*Sigma C2562*; 1:200) primary antibody was applied overnight at 4ºC followed by an incubation with a biotinylated anti-mouse IgG secondary antibody (*Vector BA-9200*; 1:200) for 1 h at room temperature. The Vector ABC kit (*Vector*) was used to amplify staining and detected using DAB (*Vector*) for brown precipitate. Hematoxylin was used to counterstain nuclei. In situ hybridization was also performed on fetal liver sections to confirm the inability for plasmid to cross the placenta and enter fetal circulation five days after treatment. All sections were imaged using the Axioscan scanning microscope (*Zeiss*).

Placenta Morphological Analysis

For placenta morphometric analyses, 5 µm thick, full-face sections were stained with Masson's trichrome stain and double-label immunohistochemistry (IHC). Sections were de-waxed and rehydrated following standard protocols. To visualize the labyrinth, sub-placenta and decidual regions, Masson's trichrome (*Sigma*) was performed as per manufacturers specifications. Whole section imaging was performed using the Axioscan Scanning Microscope (*Zeiss*) and placenta labyrinth and sub-placenta/decidua areas were measured using the Zen Imaging software (*Zeiss*). For double-label IHC, fetal capillaries and trophoblasts were distinguished using anti-vimentin

(*Dako Vim3B4*: 1:100) and anti-pan cytokeratin (*Sigma C2562*; 1:200) antibodies, respectively [27]. Antigen retrieval was performed with 0.03% protease (*Sigma*) for 15 min at 37ºC and endogenous peroxide activity was blocked with 3% hydrogen peroxide for 30 mins. The sections were then blocked with serum-free protein block (*Dako*) for 10 mins before anti-vimentin antibody was applied to slides, diluted in 10% guinea pig serum (xxx) and 1% BSA, and left overnight at 4ºC. Biotinylated anti-mouse IgG secondary antibody (*Vector BA-9200*; 1:200) was diluted in 10% guinea pig serum with 1% BSA and applied to sections for 30 mins. Antibody staining was amplified using the Vector ABC kit (*Vector*) for 40 mins and visualized using 3, 3′ diaminobenzidine tetrahydrochloride (DAB; *Vector*) with nickel to create a black precipitate. This process, from the protein block, was then repeated for anti-pan cytokeratin, however the anti-pan cytokeratin antibody remained on the sections for 2 h at room temperature and nickel was omitted from the DAB so as to form a brown precipitate. Counterstaining occurred using hematoxylin. For detailed analysis of the labyrinthine structure, the proportion of trophoblast, fetal capillaries and maternal blood space was calculated using point counting with an isotropic L-36 Merz grid [28]. Double-labeled sections were imaged using the Axioscan (*Zeiss*) and then 10 random 40x fields of view were captured. Each field of view was then counted as described in [28]. Interhaemal distance of the maternal blood space and between the maternal blood space and fetal capillaries was also calculated using the Merz grid and line intercept counting. Within-assay variation of <5% was confirmed with repeated measurement.

RNA Isolations and Quantitative PCR (qPCR)

For gene expression analysis, approximately 150-200 mg of snap frozen placenta tissue, or 50 mg fetal liver tissue was lysed in RLT-lysis buffer (*Qiagen*) with homogenization aided by a tissue-lyzer. RNA was extracted from placenta using the RNeasy Midi kit (*Qiagen*) or RNeasy Mini kit for fetal liver, and included DNase treatment, following standard manufacturers protocol. 1 µg of RNA was converted to cDNA using the High-capacity cDNA Reverse Transcription kit (*Applied Biosystems*) and diluted to 1:100. For qPCR, 2.5 µL of cDNA was mixed with 10 µL of PowerUp SYBR green (*Applied Biosystems*), 1.2 µL of primers (KiCqStart Predesigned SYBR Green Primers; *Sigma*) at a concentration of 10 nM, and water to make up a total reaction volume of 20 µL. Gene expression was normalized using housekeeping genes *β-actin*, *TBP* and *GapDH*. Reactions were performed using the StepOne-Plus Real-Time PCR System (*Applied Biosystems*), and relative mRNA expression calculated using the comparative CT method with the StepOne Software v2.3 (*Applied Biosystems*).

Statistical Analysis

All statistical analyses were performed using SPSS Statistics 26 software. Generalized estimating equations were used to determine differences between diet and nanoparticle treatment, with maternal environment treated as a random effect and gestational age as a covariate. Fetal sex was also included as a main effect but removed if no statistical significance ($P \leq 0.05$) was determined.

For statistically significant results, a Bonferroni post hoc analysis was performed. Results are reported as estimated marginal means ± standard error.

Results

Synthesis and characterization of PHPMA$_{115}$-b-PDMAEMA$_{115}$

The general schematic for the synthesis of the diblock copolymer is outlined in scheme S1 (Supplemental Material). The molar ratio of CTA and AIBN was 10:1. ^{1}H NMR spectra showed the presence of all characteristic peaks for PHPMA$_{115}$-ECT (Supplemental Figure S1). The PHPMA macro-CTA was then chain extended by RAFT block polymerization of PDMAEMA to yield the final diblock copolymer PHPMA$_{115}$-b-PDMAEMA$_{115}$. The presence of all characteristic peaks for PHPMA and PDMAEMA in ^{1}H NMR spectra confirmed successful diblock copolymer formation (Supplemental Figure S1).

The nanoparticle is rapidly endocytosed in the guinea pig placenta but only the *Cyp19a1* promotor is recognized

In order to confirm nanoparticle uptake and promotor recognition in the guinea pig placenta, a plasmid containing the GFP gene was condensed with a Texas Red conjugated polymer. 30 hours after intra-placental delivery, Texas Red fluorescence was observed in the sub-placental/decidual region of the guinea pig placenta (Figure 1), however, GFP fluorescence was only observed in placenta tissue receiving plasmid with the *Cyp19a1* promotor and not the *Plac1* promotor. There was no Texas-red fluorescence observed in the fetal liver confirming the inability for the nanoparticle to enter fetal circulation. Using qPCR, we have previously shown in mice placentas, expression of human-specific *IGF-1* following nanoparticle treatment [11, 12]. Given the high degree of homology between human and guinea pig *Igf-1*, human-specific, and therefore nanoparticle specific, *hIGF-1* expression could not be determined. However, *in situ* hybridization analysis of placenta tissue receiving the *Cyp19a1-hIGF-1* nanoparticle (NP-hIGF-1) five days after intra-placental injection, confirmed the presence of plasmid-specific mRNA in the trophoblasts of the sub-placenta/decidua region (Figure 2). Plasmid-specific mRNA was not just confined to the placenta that received the intra-placental injection, but was also found in all placentas of the litter (Supplemental Figure S2), and no positive ISH staining was found in the fetal liver further confirming the inability for plasmid to cross the placental barrier and enter fetal circulation after 5 days (Supplemental Figure S3). Analysis of guinea pig *Igf-1* mRNA revealed no expression (amplification at CT>37) in the guinea pig placenta labyrinth whilst sub-placenta/decidua expression of *Igf-1* was not altered by either diet or nanoparticle treatment ($P>0.05$; Supplemental Figure S3). Igf-1 protein, which is secreted, could not be detected in placenta tissue using IHC or Western Blot analyses (Supplemental Figure S4).

Maternal nutrient restriction reduced fetal weight but was not regulated by short term nanoparticle treatment

Fetal weight was approximately 20-25% lower in the MNR females compared to the control *ad libitum* fed females ($P<0.001$; Figure 3A). Nanoparticle treatment did not change fetal weight in

neither the control or restricted fetuses (P>0.05), but this result is unsurprising given the relative short time period between treatment and sample collection. Placenta weight was lower between MNR and control females (P=0.004; Figure 3B), however, this was largely driven by a statistically significant decrease between the control-nanoparticle and restricted-nanoparticle groups. Placenta efficiency (fetal to placental weight ratio) was not different between either diet or nanoparticle treatments (P>0.05; Figure 3C).

Nanoparticle treatment had no effect on gross placental morphology but reduced placental labyrinth interhaemal distance in the maternal nutrient restricted group

Analysis of mid-sagittal cross-sections of the placenta showed no increased signs of necrosis or gross placental defects with neither maternal nutrient restriction nor nanoparticle treatment (Figure 4). There was also no difference in the sub-placenta/decidua area (P>0.05; Figure 4A), labyrinth area (P>0.05; Figure 4B), or labyrinth weight (P>0.05; Figure 4C) with either diet or treatment. Double-label IHC was used to identify placental labyrinth trophoblast and fetal capillaries (Figure 5). Whilst nanoparticle treatment did not affect the volume density of trophoblast (P>0.05; Figure 5A) or fetal capillaries (P>0.05; Figure 5B), there was a reduction in the interhaemal distance with nanoparticle treatment, but only in the MNR group (P=0.001; Figure 5C).

Placenta nanoparticle treatment increased fetal glucose concentrations and is associated with differential mRNA expression of fetal liver glucose-sensing markers

Despite no difference in fetal weight with nanoparticle treatment, fetal glucose concentrations were approximately 50% higher in the control nanoparticle treated fetuses and approximately 38% higher in the restricted nanoparticle treated fetuses compared to sham injected (P<0.001; Figure 7A). This was associated with differential expression of Igf1 signaling and glucose-sensing genes in the fetal liver with nanoparticle treatment depending on maternal diet. Fetal liver mRNA expression of *Igf1* was lower with nanoparticle treatment (P=0.012) compared to sham injected, particularly in the control diet fetuses. *Igf1 Receptor* (*Igf1R*) mRNA expression was also decreased in control nanoparticle treated fetuses compared to control sham but not different between treatment in the restricted fetuses (Interaction P=0.02). On the other hand, fetal liver expression of *Igf Binding Protein 1* (*IgfBP1*) was increased in the restricted nanoparticle treated fetuses compared to all other groups (Interaction P<0.001), whilst *IgfBP3* expression was decreased with nanoparticle treatment in the restricted fetuses compared to restricted sham treated (Interaction P=0.033). There was a significant interaction between diet and nanoparticle treatment of *Igf2* mRNA expression (P=0.006), although no significant differences between specific groups was found with the Bonferroni post hoc analysis. In terms of glucose-sensing gene expression, fetal liver expression of *Glucose-6-Phosphatase Catalytic Subunit* (*G6pc*) was lower in the control nanoparticle treated fetuses compared to control sham (Interaction P<0.001), *Phosphoenolpyruvate Carboxykinase* (*Pck1*) mRNA expression was increased in restricted nanoparticle treated fetuses compared to restricted sham (Interaction P<0.001) and there was no difference in the expression of *Pck2*.

Discussion

In the present study, we show efficient nanoparticle uptake in the mid-pregnancy guinea pig placenta and sustained expression of human *IGF-1* in sub-placental trophoblast cells five days after nanoparticle treatment. Within this short time period, expression of *hIGF-1* in the guinea pig placenta is capable of increasing fetal blood glucose concentrations, and coupled with the observation that nanoparticle treatment reduces interhaemal distance in the growth restricted placenta but not normal placenta, indicates a potential positive effect of nanoparticle treatment on fetal growth, particularly under conditions of FGR. Additionally, we have shown changes in fetal liver gene expression of glucogenic markers with placental nanoparticle treatment dependent on fetal growth conditions that may have implications for the development of future health outcomes.

Not only does FGR significantly contribute to the rates of stillbirth and miscarriage, but is also often associated with other fetal conditions, such as congenital heart defects, in which survival from the interventional surgery after birth is largely dependent on birth weight [29]. Additionally, FGR is strongly associated with the developmental programming of adult diseases and results in permanent structural and physiological changes during fetal development that predispose the offspring to metabolic, endocrine, and cardiovascular diseases into adulthood [30]. Thus, development of an effective therapeutic to treat FGR during pregnancy is of high importance but is complicated by the need to ensure the health and safety of both mother and offspring. Our therapeutic development is designed to target the placenta and increase placental expression of *hIGF-1*, a growth factor which modulates multiple aspects of placental development and function [14]. Given that the placenta is discarded after birth, it represents the ideal site for an interventional therapy as there is no potentially long-term consequences to maternal health. Additionally, using a non-viral, biodegradable polymer deliver mechanism mitigates against concerns regarding immunogenicity and off-target affects that viral-based delivery systems have [31] as polymer-based systems have been shown to elicit less of an immune response and are safer [32-34]. Furthermore, a broad range of bioactive molecules including plasmids, siRNAs, mRNAs, proteins and oligonucleotides can be delivered with polymers [35-38] and as such, offers a promising platform for continuing to develop targeted strategies to treat the placenta and prevent FGR during pregnancy.

The importance of IGF-1 in placental development and function is well established. Through binding with the IGF-1 Receptor, it signals to increase nutrient transport across the placenta as well as modulates placental vascular development [13]. In the current study, nanoparticle treatment did not result in significant changes to fetal weight, nor gross placental morphology. However, given that the guinea pig pregnancy is 65-70 days, the lack of significant change to fetal weight is likely explained by the short time period between treatment and collection of samples. Previously, mid-pregnancy administration of IGF-1 to pregnant guinea pigs has been shown to increase placental uptake and transfer of glucose in late pregnancy [39]. However, in this study, IGF-1 was

chronically infused into the mother using an osmotic mini-pump for 18 days. In the present study, direct placental nanoparticle treatment resulted in increased fetal glucose concentrations five days after administration indicating the ability to rapidly enhance placental glucose transport to the fetus within a short period of time. Nanoparticle treatment was also capable of reducing the placental interhaemal distance between the maternal blood space and fetal circulation, albeit only in growth restricted placentas. In human term placentas, IGF-1 treatment has been shown to inhibit the release of vasoconstrictors thromboxane B_2 and prostaglandin $F_{2\alpha}$, indicating the ability for IGF-1 to enhance placental vasodilation and allow for increased blood supply to the placenta [40]. Thus, it is possible a similar mechanism is being activated in the current study, resulting in reduced interhaemal distance. Given that the change in placental morphology was only observed in growth restricted samples likely indicates a differential response of the placenta to nanoparticle treatment between normal and adverse growth conditions; under normal conditions the placental response is to prevent fetal overgrowth, whilst under adverse conditions it is to enhance fetal growth.

During fetal development, there is multi-directional communication between mother and fetus, all of which is coordinated by the placenta [41]. Nutrients, oxygen and signaling factors like hormones, are transferred across the placenta, through the umbilical cord to the liver, before reaching the fetal heart. Thus, the liver is the first organ which receives nutrient and oxygen rich blood from the placenta as well as any placental communication factors [42]. Despite confirming the inability for neither the nanoparticle, nor plasmid to cross the placenta and enter fetal circulation, there was a differential response in fetal liver expression of factors involved in gluconeogenesis to placental nanoparticle treatment depending on if the fetus was growth restricted or not. In both sheep and rat models, FGR has been associated with increased expression of gluconeogenesis markers including *G6pc*, *Pck1* and *Pck2*, as well as *IgfBP1* in the fetal liver [43-46]. In the present study, we did not observe a significant increase in expression in untreated growth restricted fetuses when compared to untreated control, however this could be due to the mid-pregnancy time point as many of the previous studies have analyzed expression near term. Under normal growth conditions, endogenous fetal glucose production is absent because glucose supply from the placenta is sufficient, however, under FGR, the fetal liver increases gluconeogenesis and thus glucose production in order to maintain vital glucose supply to the developing organs [46, 47]. Presented here, changes in expression with nanoparticle treatment dependent on whether the fetus is growth restricted or not conforms to this understanding. Decreased expression of *Igf-1*, *Igf-1R* and *G6pc* in control nanoparticle treated fetal liver compared to control sham treated indicates a down regulation in gluconeogenesis as placental supply of glucose is sufficient whilst increased expression of *IgfBP1*, *G6pc* and *Pck1* indicates upregulation of gluconeogenesis.

Our findings, that both the placenta and fetal liver responds differently to nanoparticle treatment depending on maternal environment and fetal growth highlights the huge translational potential this treatment could have in human pregnancies. Generally known as the “developmental origins

of health and disease", this phenomenon is centralized around the understanding that early environmental stressors during critical fetal developmental windows result in permanent, adaptive structural and physiologic changes that predispose the offspring to metabolic, endocrine, and cardiovascular disease in postnatal life [30]. Thus, the potential to improve fetal growth trajectories under adverse pregnancy conditions has the ability to not only improve immediate post-natal outcomes for the offspring but also life-long adult health. Furthermore, our findings indicate that administration of our therapy under normal growth conditions is unlikely to result in fetal overgrowth, which too has problematic implications for health later in life. In the present study, nanoparticle was injected directly to the placenta in order to maximize delivery and placental uptake. Clinically however, this method of delivery is sub-optimal and therefore, future studies utilizing intravenous nanoparticle delivery and enhancing the placental homing capabilities are required. Despite this, the current study shows how treatment of the placenta with a polymer-based nanoparticle causes rapid expression of *hIGF-1* in the guinea pig placenta, ultimately increasing fetal glucose concentrations within five days of treatment. Furthermore, we confirm the ability for the placenta to modulate the physiological response to nanoparticle treatment depending on maternal environment. Such outcomes provide a promising foundation for further development and futures studies of this therapy for the treatment of FGR in human pregnancies.

Declarations

Ethics approval: Animal care and usage was approved by the Institutional Animal Care and Use Committees at Cincinnati Children's Hospital and Medical Center (Protocol number 2017-0065) and University of Florida (Protocol number 202011236).

Competing Interests: The authors have declared that no competing interest exists

Funding: This study was funded by Eunice Kennedy Shriver National Institute of Child Health and Human Development (NICHD) award R01HD090657 (HNJ).

Abbreviations

FGR: fetal growth restriction; HPMA-DMEAMA: N-(2-hydroxypropyl) methacrylamide-2-(dimethylamino)ethyl methacrylate; hIGF1: human insulin-like 1 growth factor; NMR: nuclear magnetic resonance; GFP: green fluorescent protein; MNR: maternal nutrient restriction; NP: nanoparticle; G6pc: glucose-6-phosphatase catalytic subunit; Pck1: phosphoenolpyruvate carboxykinase

References

1. Resnik R. Intrauterine growth restriction. Obstet Gynecol. 2002; 99: 490-6.
2. Bamfo JE, Odibo AO. Diagnosis and management of fetal growth restriction. J Pregnancy. 2011; 2011: 640715.
3. Bernstein IM, Horbar JD, Badger GJ, Ohlsson A, Golan A. Morbidity and mortality among very-low-birth-weight neonates with intrauterine growth restriction. The Vermont Oxford Network. Am J Obstet Gynecol. 2000; 182: 198-206.

4. Crispi F, Miranda J, Gratacos E. Long-term cardiovascular consequences of fetal growth restriction: biology, clinical implications, and opportunities for prevention of adult disease. Am J Obstet Gynecol. 2018; 218: S869-S79.
5. Leitner Y, Fattal-Valevski A, Geva R, Eshel R, Toledano-Alhadef H, Rotstein M, et al. Neurodevelopmental outcome of children with intrauterine growth retardation: a longitudinal, 10-year prospective study. J Child Neurol. 2007; 22: 580-7.
6. Pritchard N, Kaitu'u-Lino Tu, Harris L, Tong S, Hannan N. Nanoparticles in pregnancy: the next frontier in reproductive therapeutics. Human Reproduction Update. 2020; 27: 280-304.
7. Bamrungsap S, Zhao Z, Chen T, Wang L, Li C, Fu T, et al. Nanotechnology in therapeutics: a focus on nanoparticles as a drug delivery system. Nanomedicine (Lond). 2012; 7: 1253-71.
8. Kim BY, Rutka JT, Chan WC. Nanomedicine. N Engl J Med. 2010; 363: 2434-43.
9. Ganguly E, Hula N, Spaans F, Cooke CM, Davidge ST. Placenta-targeted treatment strategies: An opportunity to impact fetal development and improve offspring health later in life. Pharmacol Res. 2020; 157: 104836.
10. Wilson RL, Jones HN. Targeting the Dysfunctional Placenta to Improve Pregnancy Outcomes Based on Lessons Learned in Cancer. Clin Ther. 2021.
11. Abd Ellah N, Taylor L, Troja W, Owens K, Ayres N, Pauletti G, et al. Development of Non-Viral, Trophoblast-Specific Gene Delivery for Placental Therapy. PLoS One. 2015; 10: e0140879.
12. Wilson RL, Owens K, Sumser EK, Fry MV, Stephens KK, Chuecos M, et al. Nanoparticle mediated increased insulin-like growth factor 1 expression enhances human placenta syncytium function. Placenta. 2020; 93: 1-7.
13. Fowden AL. The insulin-like growth factors and feto-placental growth. Placenta. 2003; 24: 803-12.
14. Sferruzzi-Perri AN, Sandovici I, Constancia M, Fowden AL. Placental phenotype and the insulin-like growth factors: resource allocation to fetal growth. J Physiol. 2017; 595: 5057-93.
15. Jones H, Crombleholme T, Habli M. Regulation of amino acid transporters by adenoviral-mediated human insulin-like growth factor-1 in a mouse model of placental insufficiency in vivo and the human trophoblast line BeWo in vitro. Placenta. 2014; 35: 132-8.
16. Jones HN, Crombleholme T, Habli M. Adenoviral-mediated placental gene transfer of IGF-1 corrects placental insufficiency via enhanced placental glucose transport mechanisms. PLoS One. 2013; 8: e74632.
17. Keswani SG, Balaji S, Katz AB, King A, Omar K, Habli M, et al. Intraplacental gene therapy with Ad-IGF-1 corrects naturally occurring rabbit model of intrauterine growth restriction. Hum Gene Ther. 2015; 26: 172-82.
18. Morrison JL, Botting KJ, Darby JRT, David AL, Dyson RM, Gatford KL, et al. Guinea pig models for translation of the developmental origins of health and disease hypothesis into the clinic. J Physiol. 2018; 596: 5535-69.
19. Kunkele J, Trillmich F. Are precocial young cheaper? Lactation energetics in the guinea pig. Physiol Zool. 1997; 70: 589-96.
20. Enders AC, Blankenship TN. Comparative placental structure. Adv Drug Deliv Rev. 1999; 38: 3-15.
21. Mess A. The Guinea pig placenta: model of placental growth dynamics. Placenta. 2007; 28: 812-5.
22. Hilliard J. Corpus Luteum Function in Guinea Pigs, Hamsters, Rats, Mice and Rabbits1. Biology of Reproduction. 1973; 8: 203-21.
23. Elias AA, Ghaly A, Matushewski B, Regnault TR, Richardson BS. Maternal Nutrient Restriction in Guinea Pigs as an Animal Model for Inducing Fetal Growth Restriction. Reprod Sci. 2016; 23: 219-27.
24. Sohlstrom A, Katsman A, Kind KL, Roberts CT, Owens PC, Robinson JS, et al. Food restriction alters pregnancy-associated changes in IGF and IGFBP in the guinea pig. Am J Physiol. 1998; 274: E410-6.

25. Wilson R, Lampe K, Matushewski BJ, Regnault TR, Jones HN. Time mating guinea pigs by monitoring changes to the vaginal membrane throughout the estrus cycle and with ultrasound confirmation. bioRxiv. 2020.
26. Wilson RL, Stephens KK, Lampe K, Jones HN. Sexual dimorphisms in brain gene expression in the growth-restricted guinea pig can be modulated with intra-placental therapy. Pediatr Res. 2021.
27. Sferruzzi-Perri AN, Owens JA, Pringle KG, Robinson JS, Roberts CT. Maternal Insulin-Like Growth Factors-I and -II Act via Different Pathways to Promote Fetal Growth. Endocrinology. 2006; 147: 3344-55.
28. Roberts CT, White CA, Wiemer NG, Ramsay A, Robertson SA. Altered placental development in interleukin-10 null mutant mice. Placenta. 2003; 24 Suppl A: S94-9.
29. Leirgul E, Fomina T, Brodwall K, Greve G, Holmstrom H, Vollset SE, et al. Birth prevalence of congenital heart defects in Norway 1994-2009--a nationwide study. Am Heart J. 2014; 168: 956-64.
30. Barker DJ, Osmond C. Infant mortality, childhood nutrition, and ischaemic heart disease in England and Wales. Lancet. 1986; 1: 1077-81.
31. Ahi YS, Bangari DS, Mittal SK. Adenoviral vector immunity: its implications and circumvention strategies. Curr Gene Ther. 2011; 11: 307-20.
32. Sharma R, Lee JS, Bettencourt RC, Xiao C, Konieczny SF, Won YY. Effects of the incorporation of a hydrophobic middle block into a PEG-polycation diblock copolymer on the physicochemical and cell interaction properties of the polymer-DNA complexes. Biomacromolecules. 2008; 9: 3294-307.
33. Le Bon B, Van Craynest N, Boussif O, Vierling P. Polycationic diblock and random polyethylene glycol- or tris(hydroxymethyl)methyl-grafted (co)telomers for gene transfer: synthesis and evaluation of their in vitro transfection efficiency. Bioconjug Chem. 2002; 13: 1292-301.
34. Andersen MO, Howard KA, Paludan SR, Besenbacher F, Kjems J. Delivery of siRNA from lyophilized polymeric surfaces. Biomaterials. 2008; 29: 506-12.
35. Alinejad V, Hossein Somi M, Baradaran B, Akbarzadeh P, Atyabi F, Kazerooni H, et al. Co-delivery of IL17RB siRNA and doxorubicin by chitosan-based nanoparticles for enhanced anticancer efficacy in breast cancer cells. Biomed Pharmacother. 2016; 83: 229-40.
36. Navarro G, Pan J, Torchilin VP. Micelle-like nanoparticles as carriers for DNA and siRNA. Mol Pharm. 2015; 12: 301-13.
37. Teo PY, Cheng W, Hedrick JL, Yang YY. Co-delivery of drugs and plasmid DNA for cancer therapy. Adv Drug Deliv Rev. 2016; 98: 41-63.
38. Duvall CL, Convertine AJ, Benoit DS, Hoffman AS, Stayton PS. Intracellular delivery of a proapoptotic peptide via conjugation to a RAFT synthesized endosomolytic polymer. Mol Pharm. 2010; 7: 468-76.
39. Sferruzzi-Perri AN, Owens JA, Standen P, Taylor RL, Heinemann GK, Robinson JS, et al. Early treatment of the pregnant guinea pig with IGFs promotes placental transport and nutrient partitioning near term. Am J Physiol Endocrinol Metab. 2007; 292: E668-76.
40. Siler-Khodr TM, Forman J, Sorem KA. Dose-related effect of IGF-I on placental prostanoid release. Prostaglandins. 1995; 49: 1-14.
41. Murphy VE, Smith R, Giles WB, Clifton VL. Endocrine regulation of human fetal growth: the role of the mother, placenta, and fetus. Endocr Rev. 2006; 27: 141-69.
42. Godfrey KM, Haugen G, Kiserud T, Inskip HM, Cooper C, Harvey NC, et al. Fetal liver blood flow distribution: role in human developmental strategy to prioritize fat deposition versus brain development. PloS one. 2012; 7: e41759.
43. Gentili S, Morrison JL, McMillen IC. Intrauterine growth restriction and differential patterns of hepatic growth and expression of IGF1, PCK2, and HSDL1 mRNA in the sheep fetus in late gestation. Biol Reprod. 2009; 80: 1121-7.
44. Yoon JC, Puigserver P, Chen G, Donovan J, Wu Z, Rhee J, et al. Control of hepatic gluconeogenesis through the transcriptional coactivator PGC-1. Nature. 2001; 413: 131-8.

45. Jones AK, Brown LD, Rozance PJ, Serkova NJ, Hay WW, Jr., Friedman JE, et al. Differential effects of intrauterine growth restriction and a hypersinsulinemic-isoglycemic clamp on metabolic pathways and insulin action in the fetal liver. Am J Physiol Regul Integr Comp Physiol. 2019; 316: R427-R40.
46. Thorn SR, Brown LD, Rozance PJ, Hay WW, Jr., Friedman JE. Increased hepatic glucose production in fetal sheep with intrauterine growth restriction is not suppressed by insulin. Diabetes. 2013; 62: 65-73.
47. Jones AK, Rozance PJ, Brown LD, Goldstrohm DA, Hay WW, Jr., Limesand SW, et al. Sustained hypoxemia in late gestation potentiates hepatic gluconeogenic gene expression but does not activate glucose production in the ovine fetus. Am J Physiol Endocrinol Metab. 2019; 317: E1-E10.

Figures

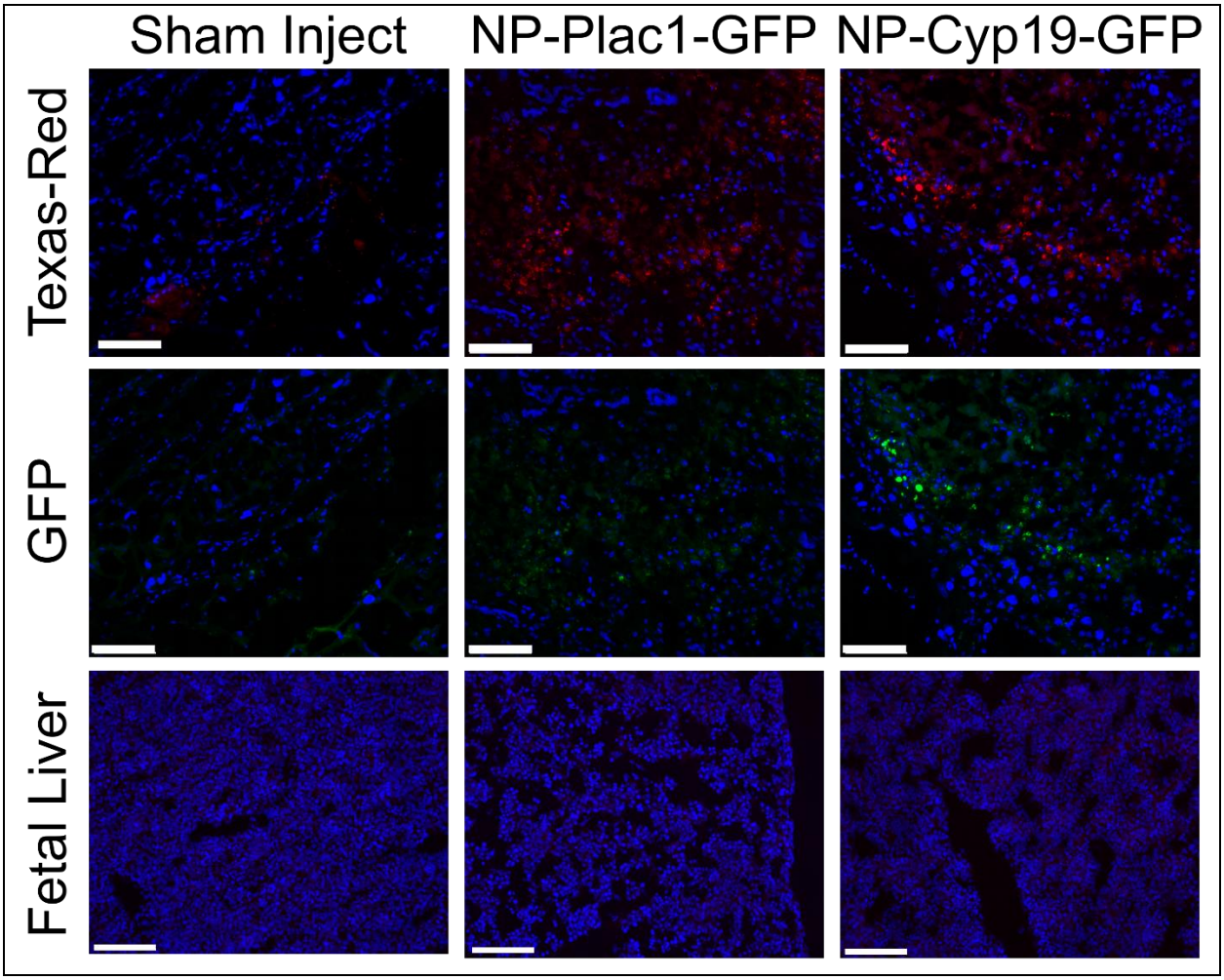

Figure 1 Fluorescent microscopy of nanoparticle (NP-Plac1-GFP and NP-Cyp19-GFP) localization and transgene expression in the guinea pig placenta and fetal liver. Conjugation of the HPMA-DMEAMA copolymer with a Texas Red fluorophore (Red) [12] confirmed nanoparticle uptake in the guinea pig placenta 30 h after intra-placental injection. Analysis of green fluorescent protein (GFP; Green) fluorescence showed only the Cyp19, and not the Plac1, promotor was recognized by guinea pig trophoblast cells. Fluorescence of neither Texas Red nor GFP was found in fetal liver tissue confirming the inability for nanoparticle to cross the

placenta and enter fetal circulation. Nuclei counter-stained with Dapi (Blue). Scale bar = 0.1 mm.

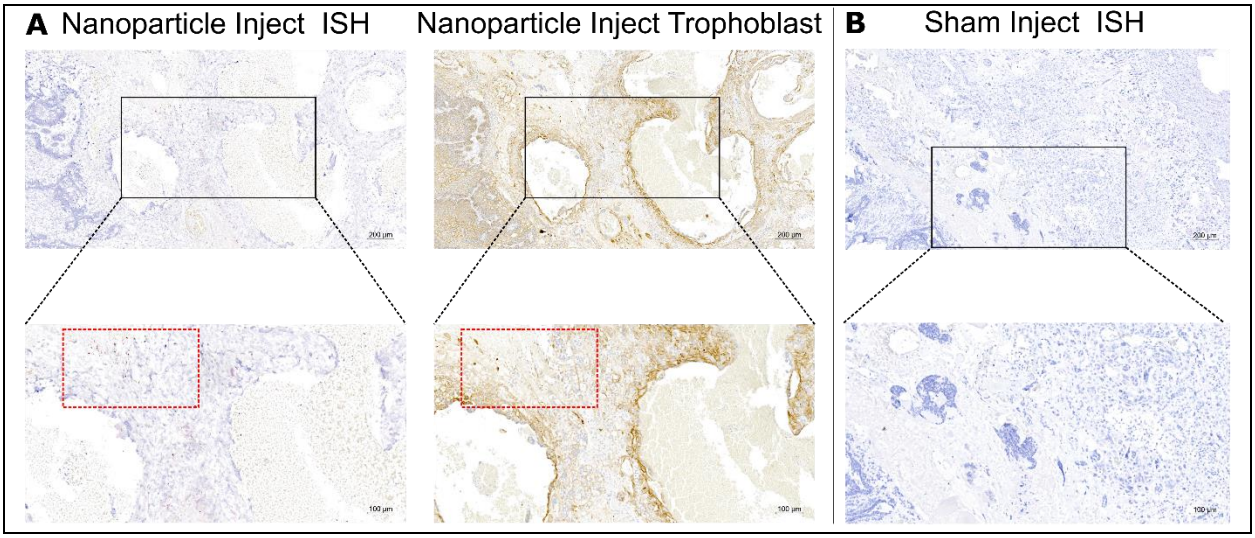

Figure 2 In situ hybridization (ISH) for plasmid-specific mRNA expression in the guinea pig placenta five days after intra-placental nanoparticle treatment. ISH confirmed transgene expression in the guinea pig sub-placenta/decidua five days after nanoparticle treatment (**A first panel**). Serial sectioning and immunohistochemistry confirmed plasmid-specific mRNA was localized to trophoblast cells (anti-pan cytokeratin; **A second panel**). Sham injected tissue was used as a negative control and no positive staining for plasmid-specific mRNA was observed (**B**). Scale bar top row = 200 µm, scale bar bottom row = 100 µm

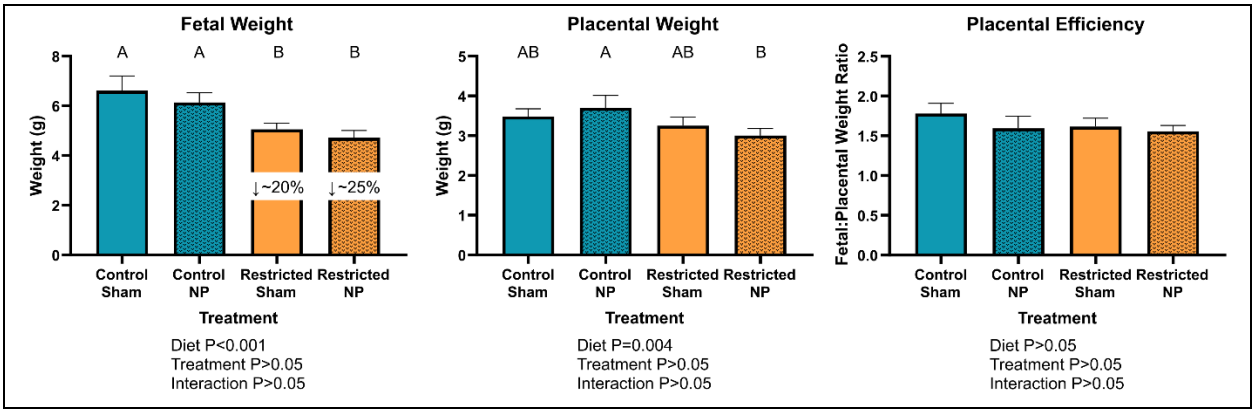

Figure 3 Effect of maternal nutrient restriction (MNR) diet and nanoparticle treatment on mid-pregnancy fetal and placental weight. MNR resulted in approximately 20-25% reduction in fetal weight at mid-pregnancy and there was no effect of nanoparticle treatment in either the control or growth restricted fetuses (**A**). Irrespective of nanoparticle treatment, MNR reduced placental weight at mid-pregnancy, although it was only the control-nanoparticle treated and restricted-nanoparticle treated placentas that were significantly different (**B**). There was no difference in placental efficiency (fetal placental weight ratio) with either MNR diet or nanoparticle treatment

(**C**). *n* = 7 control-sham females (21 fetuses/placentas), 4 control-nanoparticle females (12 fetuses/placentas), 5 restricted-sham females (14 fetuses/placentas) and 7 restricted-nanoparticle females (19 fetuses/placentas). Data are estimated marginal means + standard error. P values calculated using generalized estimating equations with Bonferroni post hoc analysis. Different letters denote a significant difference of P<0.05.

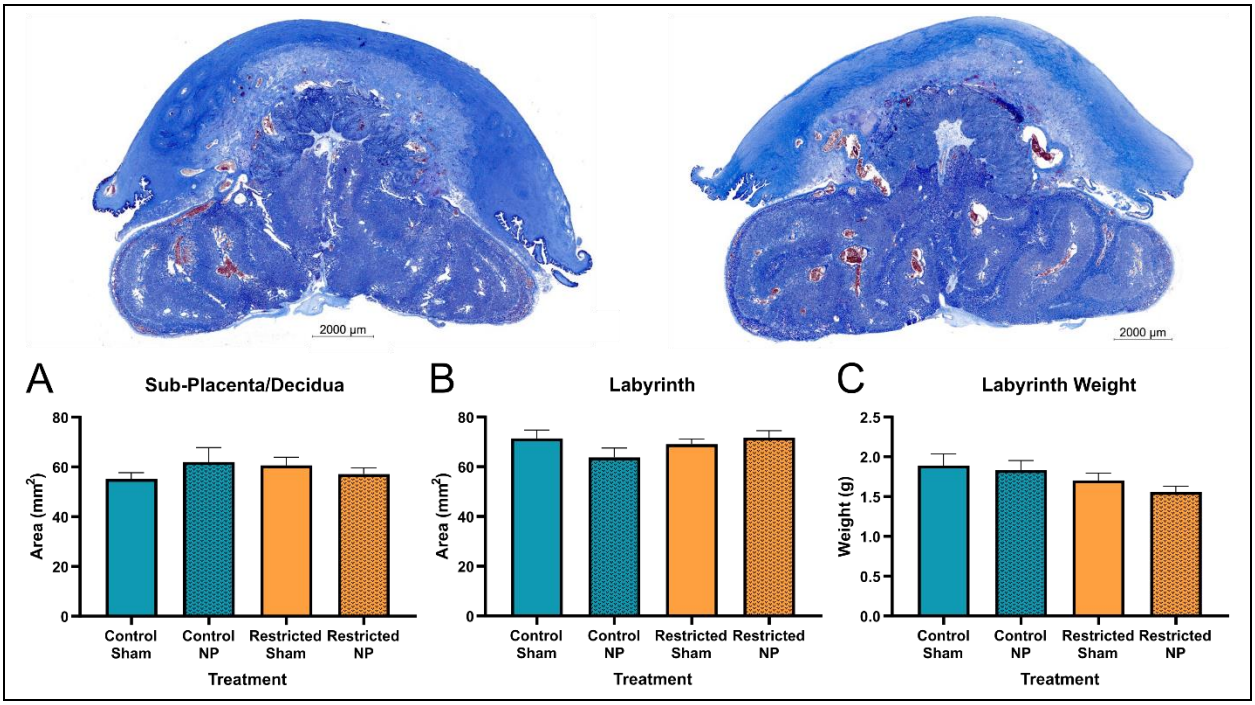

Figure 4 Effect of maternal nutrient restriction (MNR) diet and nanoparticle treatment on mid-pregnancy gross placental morphology. There were no indicators of increased necrosis or inflammation in the placenta with intra-placental treatment. Neither MNR diet nor nanoparticle treatment effected sub-placenta/decidua area (**A)**, labyrinth area (**B)**, nor labyrinth weight (**C**). Images are representative mid-sagittal cross sections of a control nanoparticle treated placenta (left) and restricted nanoparticle treated placenta (right). *n* = 7 control-sham females (21 placentas), 4 control-nanoparticle females (12 placentas), 5 restricted-sham females (14 placentas) and 7 restricted-nanoparticle females (19 placentas). Data are estimated marginal means + standard error. P values calculated using generalized estimating equations with Bonferroni post hoc analysis.

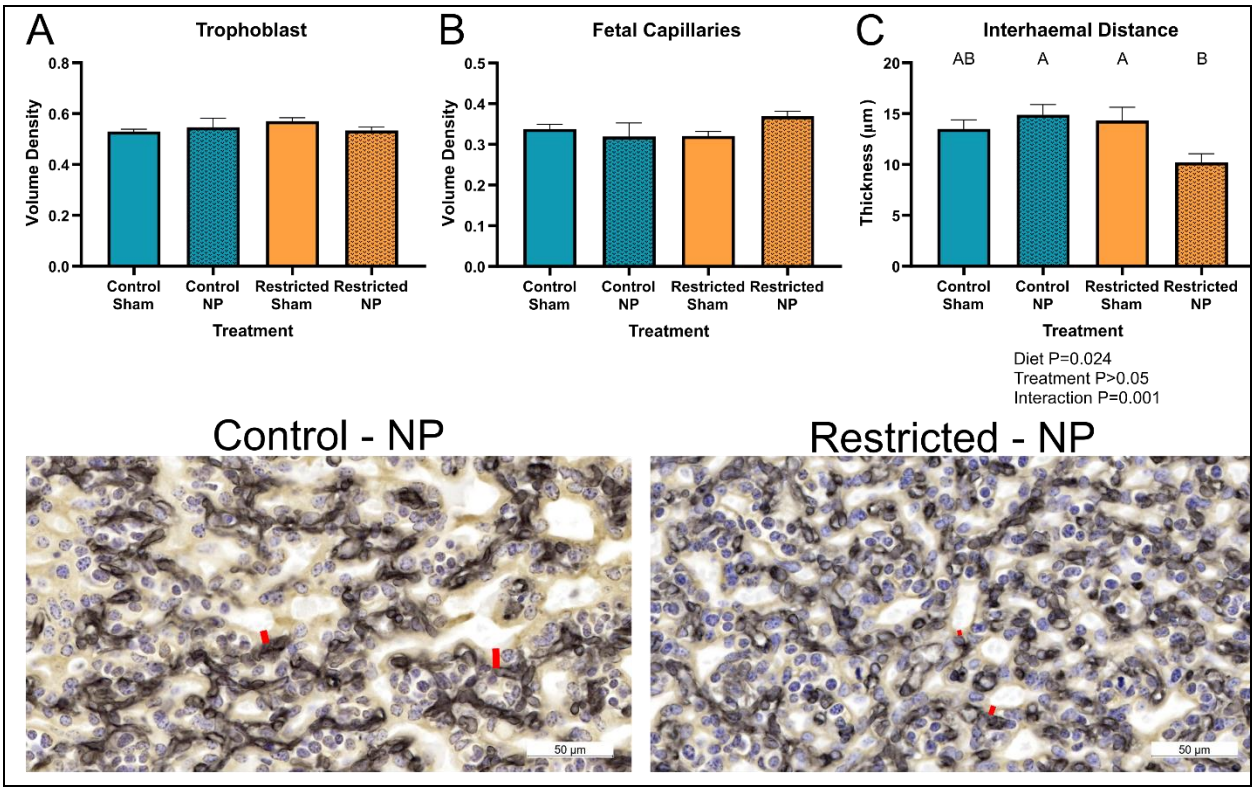

Figure 5 Effect of maternal nutrient restriction (MNR) diet and nanoparticle treatment on mid-pregnancy placenta microstructure. There was no change to the volume densities of neither the trophoblast (**A)** or fetal capillary cells (**B)** within the placental labyrinth with either MNR or nanoparticle treatment. Nanoparticle did however, differentially affect the interhaemal distance (distance between maternal blood space and fetal circulation) depending on MNR diet (**C**). Nanoparticle treatment resulting in a significant reduction in interhaemal distance in the growth restricted placentas compared to growth restricted-sham treated but did not affect control diet placentas when compared to sham treated. Representative images of double-label immunohistochemistry identifying trophoblast (pan-cytokeratin: brown) and fetal capillary cells (vimentin: black) in the labyrinth of control-nanoparticle and growth restricted-nanoparticle treated placentas. Red bars indicate interhaemal distance. n = 7 control-sham females (21 placentas), 4 control-nanoparticle females (12 placentas), 5 restricted-sham females (14 placentas) and 7 restricted-nanoparticle females (19 placentas). Data are estimated marginal means + standard error. P values calculated using generalized estimating equations with Bonferroni post hoc analysis. Different letters denote a significant difference of $P<0.05$.

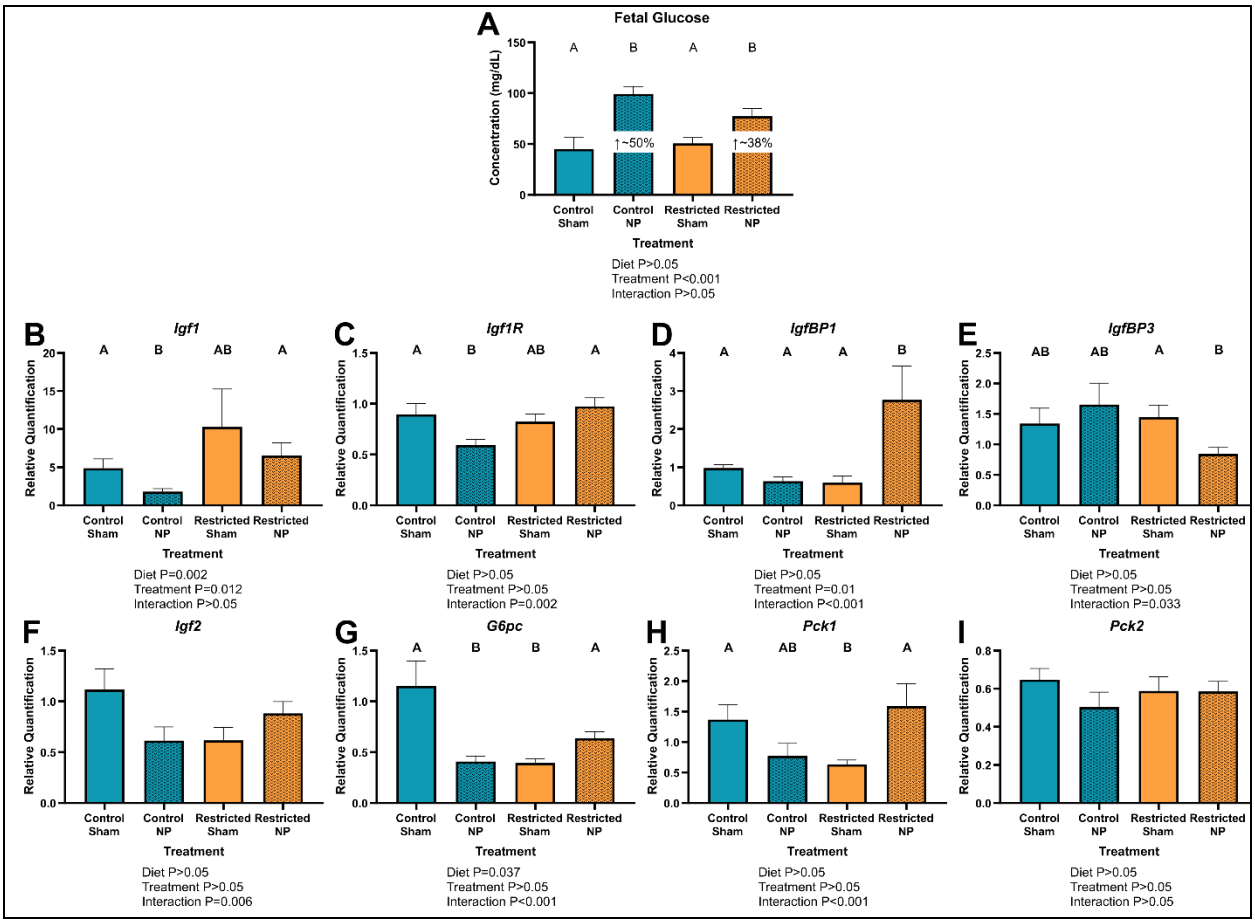

Figure 6 Effect of maternal nutrient restriction (MNR) diet and nanoparticle treatment on fetal blood glucose concentrations and fetal liver gene expression in mid-pregnancy. Irrespective of diet, placental nanoparticle treatment increased fetal blood glucose concentrations by approximately 38-50% (**A**). Fetal liver mRNA expression of *insulin-like 1 growth factor* (*Igf1*), irrespective of nanoparticle treatment was increased in the MNR samples and decreased with nanoparticle treatment irrespective of diet (**B**). There was a differential effect of nanoparticle treatment on fetal liver mRNA expression, depending on diet of *Igf1 Receptor* (*Igf1R*: **C**), *Igf Binding Protein 1* (*IgfBP1*: **D**), *IgfBP3* (**E**), *Igf2* (**F**), *Glucose-6-Phosphatase Catalytic Subunit* (*G6pc*: **G**) and *Phosphoenolpyruvate Carboxykinase* (*Pck1*: **H**). There was no effect of neither MNR diet nor nanoparticle treatment on fetal liver mRNA expression of *Pck2* (**I**). *n* = 6 control-sham females (14 fetuses), 4 control-nanoparticle females (11 fetuses), 5 restricted-sham females (10 fetuses) and 7 restricted-nanoparticle females (17 fetuses). Data are estimated marginal means + standard error. P values calculated using generalized estimating equations with Bonferroni post hoc analysis. Different letters denote a significant difference of P<0.05.